

This work was written as part of one of the author's official duties as an Employee of the United States Government and is therefore a work of the United States Government. In accordance with 17 U.S.C. 105, no copyright protection is available for such works under U.S. Law.

Public Domain Mark 1.0

<https://creativecommons.org/publicdomain/mark/1.0/>

Access to this work was provided by the University of Maryland, Baltimore County (UMBC) ScholarWorks@UMBC digital repository on the Maryland Shared Open Access (MD-SOAR) platform.

Please provide feedback

Please support the ScholarWorks@UMBC repository by emailing scholarworks-group@umbc.edu and telling us what having access to this work means to you and why it's important to you. Thank you.

PROCEEDINGS OF SPIE

[SPIDigitalLibrary.org/conference-proceedings-of-spie](https://spiedigitallibrary.org/conference-proceedings-of-spie)

Comparisons of USDA UV shadow-band irradiance measurements with TOMS satellite and DISORT model retrievals under all sky conditions

James Slusser, Nickolay Krotkov, Wei Gao, Jay Herman, Gordon Labow, et al.

James R. Slusser, Nickolay A. Krotkov, Wei Gao, Jay R. Herman, Gordon Labow, Gwen Scott, "Comparisons of USDA UV shadow-band irradiance measurements with TOMS satellite and DISORT model retrievals under all sky conditions," Proc. SPIE 4482, Ultraviolet Ground- and Space-based Measurements, Models, and Effects, (17 January 2002); doi: 10.1117/12.452954

SPIE.

Event: International Symposium on Optical Science and Technology, 2001, San Diego, CA, United States

Comparisons of USDA UV shadow-band irradiance measurements with TOMS satellite and DISORT model retrievals under all sky conditions

J. R. Slusser^{*1 a}, N. Krotkov^b, W. Gao^c, J. R. Herman^d, G. Labow^e, and G. Scott^a

^aNatural Resource Ecology Laboratory, Colorado State University, Fort Collins, CO

^bGoddard Earth Science and Technology Center, University of Maryland Baltimore County, MD

^cCooperative Institute for Research in the Atmosphere, Colorado State University, Fort Collins, CO

^dNASA Goddard Space Flight Center, Greenbelt, MD

^eSAIC, Greenbelt, MD

ABSTRACT

Comparisons of UV irradiances measured by the USDA UVB Monitoring and Research Network at 305- and 368-nm with retrievals from the NASA TOMS and a multiple scattering radiative transfer code were made for an 18-month period from January 1, 2000 through May 31, 2001 for Las Cruces, New Mexico, USA (32.6°N, 106.7°W, 1317 m elevation) and Billings, Oklahoma, USA (36.6°, 97.5°W, 317 m elevation). Agreement is generally within $\pm 12\%$ for all sky conditions and 8% for clear skies. The effects of aerosols is mostly $< 5\%$, consistent with the measured aerosol optical depths at 368 nm within the range of 0.05 and 0.25.

Keywords: Solar ultraviolet radiation, transmission, total column ozone

1. INTRODUCTION

Concern over the harmful effects of increased UVB on the biosphere has prompted efforts to determine its intensity at the earth's surface. For this purpose, various government agencies have set up programs to measure UV at the ground using broad-band and narrow-band radiometers as well as spectrometers. To make these measurements meaningful, strict observance to quality control of data, and regular and accurate calibrations are required. However to construct the UV climatologies required by effects researchers in agricultural, human health, and materials degradation, spatial interpolation between these geographically sparse sites is needed. To provide this continuous spatial coverage, there has been considerable effort to develop satellite UV retrievals. The previous work¹⁻²⁰ is summarized in Table 1. Ground-based measurements and satellite retrievals complement each other by identifying biases and combining the best features of both (e.g. frequent measurements of radiation that actually reach the earth for ground-based measurements and total spatial coverage from a single platform for satellites). Satellite UV retrieval schemes typically use a radiative transfer model with inputs the total column ozone, surface albedo, and the attenuation due to clouds and aerosols relative to clear-skies. Variations in sky transmission due to changes in ozone are relatively slow, so a single daily ozone reading is normally sufficient. Conversely, the optical properties of clouds and aerosols change rapidly leading to huge variations in sky transmission within a day. Since polar orbiters such as the NASA Total Ozone Mapping Spectrometer (TOMS) make only a one near-noon overpass per day, its ability to determine C_T is limited and time averaging of ground-based measurements must be employed for comparisons²⁰. Other UV retrieval schemes use TOMS to determine ozone and evaluate C_T from geostationary satellites that allow multiple determinations of C_T throughout the day⁹. Since a well calibrated and characterized ground based radiometer makes frequent measurements of the UV that actually passes through the atmosphere, whereas satellite retrievals use a model with estimated transmission parameters as input, there will always be the

^{*1}sluss@uvb.nrel.colostate.edu; Telephone (970) 491-3623

need to have well calibrated ground based measurements of UV. It is the purpose of this study to compare UV ground-based measurements of total horizontal irradiance at 305- and 368-nm with simulations from a standard multiple scattering model and the TOMS retrievals. To minimize the effects due to clouds, a desert site in the North America was selected: Las Cruces, New Mexico (32.6°N, 106.7°W, 1317 m elevation). A cloudy and humid continental site was also chosen to study cloud effects: Billings, Oklahoma (36.6°, 97.5°W, 317 m elevation). The uncertainties in calibration, stability, and cosine response of the ground-based measurements, as well as possible biases in the satellite retrievals due to aerosols, clouds, and snow will be explored.

Table 1: Research in Satellite UV Retrievals

Author(s)	Date	Reference
Frederick and Lubin	1988	1
Madronich	1992a	2
Madronich and Granier	1992b	3
Madronich and de Gruijl	1993	4
Eck et al.	1995	5
Herman et al.	1996	6
Herman et al.	1999	7
Long et al.	1996	8
Meerkötter et al.	1997	9
Lubin et al.	1998	10
Madronich et al.	1998	11
Mayer et al.	1998	12
Krotkov et al.	1998	13
Udelhofen et al.	1999	14
Soulen and Frederick	1999	15
Wang et al.	2000	16
Kalliskota et al.	2000	17
Matthijsen et al.	2000	18
Verdebout	2000	19
Krotkov et al.	2001	20

2. INSTRUMENTATION

The USDA UVB Monitoring and Research Network²¹ measures UV and other relevant parameters at 28 US and two Canadian sites. The primary instrument is the ultra-violet multi-filter rotating shadow-band radiometer (UV-MFRSR) which measures total horizontal, direct, and diffuse irradiances at 7 UV wavelengths: 300- 305-, 311-, 317-, 325-, 332-, and 368-nm with a full-width at half maximum of about 2.0 nm.

Calibration of the detectors is performed by the NOAA Central Ultraviolet Calibration Facility (CUCF) using 1000-W NIST-traceable lamps²². The spectral response of every radiometer's 7 channels is measured by the CUCF to within an accuracy of 0.02 nm. Radiometric stability of the detectors is monitored in the field using a time series of Langley plot voltage intercepts²³. Figure 1 (left) shows a time series of the voltage intercepts for the 305- and 368-nm channels for the radiometer from the New Mexico site. The approximate drift per year, determined by the least squares slope of the voltage intercept time series, is shown in Figure 1 (right) to be less than 4% for all channels. The angular or cosine response of the detectors is measured by Yankee Environmental Systems²¹, and direct beam and diffuse corrections applied using the isotropic sky assumption²⁴. The total absolute radiometric uncertainty is estimated at $\pm 5.2\%$ and summarized in Table 2.

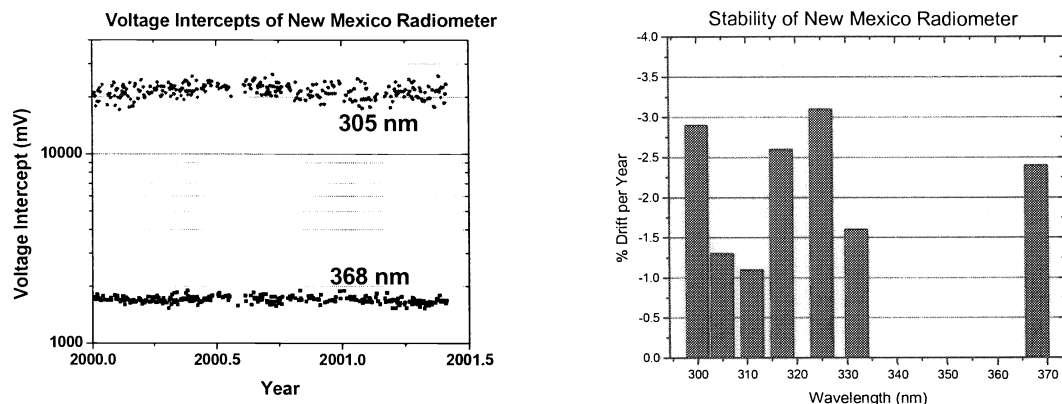


Figure 1: The left plot shows a time series of the Langley voltage intercepts for the 368- and 305- nm channels for the New Mexico radiometer. The right histogram shows the estimated change in each channel's sensitivity as determined by a least-squares fit of the time series.

Table 2: USDA ground-based radiometer uncertainty budget

Factor	Estimated uncertainty
Initial lamp Absolute response calibration	< 3%
Initial Spectral Response characterization	< 0.02 nm
Spectral stability	< 0.02 nm
Absolute response stability	< 3%
Stray light rejection	< 0.5%
Initial Cosine response characterization	< 2%
Cosine response and corrections	< 2%
Linearity	< 1%
Field of view of site	< 1%
Total Estimated Uncertainty	< 5.2%

The TOMS Earth-Probe (TOMS / EP), launched in 1996, is described by Herman et al⁷. The satellite measures back scattered radiances at 6 UV wavelengths with a field of view of 3 degrees resulting in a pixel size of between 40 and 160 km depending on orbital look angle. In-space calibration is accomplished by viewing the sun using 3 diffuser plates that are exposed for different total amounts of time. Some reasons for satellite UV retrieval uncertainties are: calibration and stability of the detector, pixel to single point match-up, time averaging, the effects of non-absorbing and absorbing aerosols, continuous and broken clouds, snow over, tropospheric ozone, and the temperature dependence of ozone cross sections.

3. MODELS USED

The discrete ordinate multiple scattering code (DISORT) of Stamnes et al.²⁵ with a user-friendly interface by Madronich²⁶ was run using 8 streams with no clouds or aerosols. Column ozone was determined from the direct-Sun as described by Gao et al.²⁷ (2001) and irradiances determined by linear interpolation. The model was run in increments of 0.1 nm, 10 DU, 0.1 km, and 5° solar zenith angle (SZA). The ozone cross section of Molina and Molina and corrected to simulate the ozone cross sections of Bass and Paur used by TOMS. The measured spectral

response function of the actual radiometer channel was then passed over the model irradiance to generate the simulated irradiance. A previous comparison of DISORT with spectral UV measurements by Zeng et al.²⁸ showed satisfactory agreement was hampered by the poorly known extraterrestrial solar flux. In the current study, the extraterrestrial solar flux from the Space Shuttle Atlas 3 flight using the SUSIM spectrometer was used and corrected for vacuum to air. The improved accuracy of this spectrum was recently validated by Gröbner and Kerr²⁹. Surface albedo was fixed at 0.05 independent of wavelength according to measurements by McKenzie et al.³⁰. Measurements at 5° increments of SZA were compared with model simulations. Clear sky days were identified by days yielding both morning and afternoon Langley plots as described by Harrison and Michalsky³¹. The estimated DISORT model uncertainty budget for a clear sky and an aerosol optical of 0.20 at 368 nm is shown in Table 3.

Table 3: Estimated Model Uncertainty Budget at 305nm

Factor	Estimated uncertainty	Irradiance uncertainty
Extraterrestrial solar flux	–	3 %
Surface albedo	0.02	1 %
Surface pressure	30 mb	2 %
Column ozone	6 DU	3.5%
Aerosol optical depth	0.02	1 %
Aerosol single scattering albedo	0.10	3.3%
Aerosol asymmetry parameter	0.10	1 %
Ozone cross sections (Molina and Molina vs Bass and Paur)	--	3 %
Temperature profile	10°C	2.6%
Ozone profile	-	<1%
Aerosol profile	--	<1%
Total Estimated Uncertainty		<7.2%

The TOMS UV retrievals used Rayleigh lookup tables, TOMS determined ozone and C_T (cloud transmittance)²⁰ and shifted Atlas 3 SUSIM extraterrestrial solar flux²⁹. To account for clouds, the USDA measurements ± 1 hour of the satellite overpass were averaged to compare with the TOMS retrievals. Multiple satellite retrievals for each day were included if available.

The operational TOMS UV algorithm does not distinguish between water clouds, haze, ice clouds and non-absorbing aerosols. To estimate the cloud / aerosol correction at the overpass time the TOMS algorithm uses a homogeneous cloud model embedded into a Rayleigh scattering atmosphere with known ozone absorption and surface reflectivity assuming 100% cloud cover²⁰. For snow-free conditions in the near UV spectral region surface albedo is uniformly low and can be accurately predicted from a climatological data base that was developed using 15 years of TOMS data³². The “effective” cloud / aerosol optical thickness is derived by matching the measured 360 nm radiance at the overpass time with the calculated radiance for each TOMS/EP field of view.

Treating non-absorbing aerosol as thin cloud of the same reflectance could result in a few percent overestimation of surface UV irradiance. On the other hand, a significantly larger overestimation occurs if absorbing aerosol (smoke, dust) is present, but is treated as non-absorbing or cloud. When absorbing aerosol plumes are detected in the TOMS Aerosol Index (AI) data the cloud correction is replaced by the Absorbing Aerosol Correction (AAC) algorithm^{7, 13}. However, the initial AAC algorithm¹³ can not be applied for mountain sites and should be corrected for the actual terrain pressure. The correction was not available at the time of writing this paper, so we have chosen not to apply the AAC algorithm for the New Mexico site.

4. RESULTS

Since aerosols are known to attenuate UV radiation¹³, average morning and afternoon aerosol optical depths were obtained from direct-Sun Langley slopes as described by Shaw³³. Figure 2 (left plot) shows the measured aerosol optical depths at 368- and 332-nm for the site in New Mexico. The right-side plot shows the same for the site in Oklahoma.

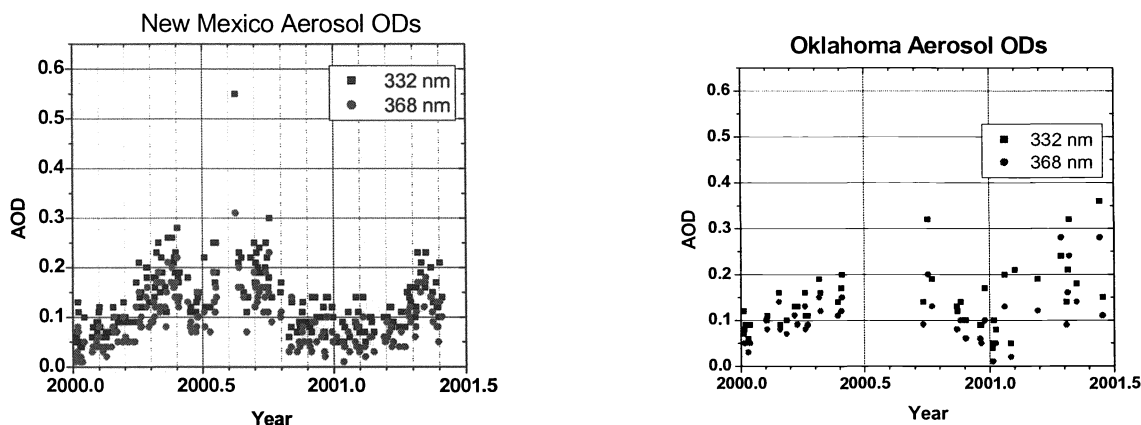


Figure 2: The left plot shows the measured aerosol optical depths at 368- and 332-nm for the site in New Mexico. The right plot shows the same for the site in Oklahoma.

Figure 3 (the remaining figures are found following the text) shows comparisons of USDA measurements versus the DISORT model with no clouds or aerosols. The top left graph is for 305 nm and top right graph is for 368 nm both for all sky conditions. The bottom left graph shows 305 nm and the bottom right the 368 nm both for clear sky. The clear sky correlation, R^2 , is excellent (0.99 at 305 nm and 0.98 at 368 nm), with the slope of the regression line 0.84 at 305 nm and 0.94 at 368 nm. Thus the model overestimates the measurement at 305 nm but is within error bars at 368 nm. Possible causes for this discrepancy will be explored in the Discussion section below.

Comparisons of USDA measurements versus the TOMS retrieval for the New Mexico site are shown in Figure 4. The top left graph is for 305 nm and top right graph is for 368 nm (both all sky conditions). The bottom left graph shows 305 nm and bottom right the 368 nm comparisons (both clear sky). Again the correlations for clear sky are excellent (0.98 at 305 nm and 0.97 at 368 nm) and the slope of the regression line is 0.95 at 305 nm and 0.88 at 368 nm. It should be pointed out that for all TOMS clear sky comparisons, the TOMS algorithm determines an appropriate value of C_T that is not necessarily equal to unity.

Figure 5 shows the comparisons of USDA measurements versus the DISORT model for Oklahoma site. The top left graph is for 305 nm and the top right graph is for 368 nm (all sky conditions). The bottom left graph shows 305 nm and the bottom right 368 nm both (clear sky). Correlation for clear skies is again excellent (0.99 at 305 nm and 0.97 at 368 nm) and the slope of the regression line is 0.89 at 305 nm and 0.88 at 368 nm.

Figure 6 shows comparisons of the USDA measurements versus the TOMS retrievals for the Oklahoma site. The top left graph is for 305 nm and top right graph is for 368 nm (all sky conditions). The bottom left graph shows 305 nm and the bottom right graph 368 nm (both clear sky). Correlations for clear skies are not so good (0.85 at 305 nm and 0.60 at 368 nm) and the slope of the regression line is 0.97 at 305 nm and 0.81 at 368 nm.

Since both snow and clouds increase TOMS measured reflectivity, there is no way to separate the effects of snow from clouds based on single TOMS reflectivity measurement. In absence of external snow information the current TOMS algorithm uses a climatological snow/ice flag (probability of the presence of snow on a given day at a given location) to detect the presence of snow and climatological monthly minimal Lambert equivalent surface reflectivity

(MLER) global database³² to approximate snow albedo (A). For locations with infrequent snow cover (New Mexico, Oklahoma) TOMS assumes no snow on the ground, thus, surface albedo is low (a few percent). Therefore, for such locations TOMS tends to assign all measured reflectivity to clouds, even for snow days, thus underestimating surface UV. The error in estimated surface UV varies with snow albedo and cloud regime as quantified by Krotkov et al²⁰. The error is greatest for a fresh snow (high A) on cloud-free days (largest error in A). An example of the TOMS snow error can be seen from figure 7 which is a time series of USDA measurements and TOMS retrievals for the Oklahoma site. According to USDA downward pointing broad band radiometer data, there was a definite snow cover at Oklahoma on Dec 13 - 17, Dec 27 - 30, 2000, and Jan 1 - 5, 2001, whereas TOMS assumes no snow. These are exactly the days with greatest underestimation of surface UV by TOMS. The snow error will be corrected in the second version of the TOMS UV algorithm as discussed by Krotkov et al [this issue]. For the current paper, snow days were not excluded from the correlation analysis and adds to the overall bias.

There can be also errors in the ground-based instruments that affect comparisons. The unavoidable degradation of some optical heads of the UV-MFRSR instruments results in decreasing radiometric sensitivity with time. Comparison with well-calibrated TOMS instrument easily reveals degradation of the ground based instrument on a moderate time scales (months to years). The USDA network addresses changes in radiometric sensitivity by re-calibrating optical heads of its field instruments. This results in replacing optical heads from time to time. Until June 5, 2000 the optical head #389 was used with the UV-MFRSR at the Oklahoma site. At the end of its field cycle the head #389 had drifted downward relative to TOMS by more than 20%. On June 5, 2000, head #389 was replaced with a freshly calibrated head #299. This new head showed excellent agreement with TOMS data until late fall 2000, when snow affected comparisons as discussed above.

Table 4: Clear Sky Comparisons

DISORT					TOMS		
site	wl (nm)	slope	n	R ²	slope	n	R ²
NM	368	0.95	3992	0.98	0.88	478	0.97
	305	0.84	3992	0.99	0.95	478	0.98
OK	368	0.88	680	0.97	0.60	111	0.81
	305	0.89	680	0.99	0.85	111	0.97

5. DISCUSSION

A summary of the clear sky comparisons is shown in Table 4. Figure 8 (top graph) shows model results of the attenuation of the total, diffuse, and direct horizontal irradiances as a function of aerosol optical depth for a single scattering albedo of 0.90. As shown by Krotkov¹³, the attenuation is nearly linear with aerosol optical depth, and the slope becomes steeper for smaller values of the aerosol single scattering albedo. Figure 8 (middle graph) shows the spectral attenuation of the total horizontal irradiance for an aerosol optical depth of 0.20 and Ångström exponent of 1 for aerosol single scattering albedo values of 0.995, 0.90, and 0.80. It can be seen that the aerosol single scattering albedo has a large effect on the amount of attenuation for a given aerosol optical depth. Figure 8 (bottom graph) shows the spectral dependence of the slope of the clear sky regression line of measurements compared with the DISORT model for the New Mexico site. The spectral attenuation indicated by the slopes at 368 and 332 nm are about 0.95, but decrease rapidly with shorter wavelengths. Comparing the middle and bottom graphs points to two possibilities: either there is too much ozone attenuation at the shorter wavelengths or the aerosol attenuation increases at shorter wavelengths. But in Table 4 at the Oklahoma site there are similar slopes for the DISORT to measurement regression slopes at 305 and 368 (0.89 and 0.88 respectively) which strongly suggests that increased

attenuation due to ozone is not the reason for the large attenuation at shorter wavelengths at the New Mexico site. Therefore we hypothesize that aerosols at the New Mexico site increase in absorption at shorter wavelengths due to a smaller aerosol single scattering albedo.

6. CONCLUSIONS

Good agreement (correlation slopes to within 11%) between the clear sky measurements and the TOMS retrievals at the New Mexico site, within the combined uncertainties of both methods at 368 nm and 305 nm, gives confidence in the measurement accuracy and satellite UV retrievals for a sunny non-turbid site. At the New Mexico site, agreement of measurements to DISORT is excellent at 368 nm but at 305 nm the model underestimates. We note that regression slopes between the measurements and DISORT at Oklahoma site under clear skies are nearly the same at 305- and 368-nm which suggests larger aerosol absorption due to a smaller aerosol single scattering albedo is the cause of the larger attenuation at shorter wavelengths at the New Mexico site.

Agreement between all sky condition measurements and TOMS at Oklahoma (correlation slopes to within 20%) shows the effects of greater cloudiness, aerosol loading, and snow cover. TOMS underestimates at 368 nm (slope = 0.60) which is probably due to the drop in responsivity in radiometer #389, occasional snow cover and the difficulty of the satellite algorithm's ability to capture the actual local cloud field. Treating broken cloud fields will require multiple-site UV measurements of cloud optical depths within the TOMS pixel. Uncertainties due to clouds, snow, and UV-absorbing aerosols are the largest sources of systematic error in determining surface UV from space.

ACKNOWLEDGMENTS

Thanks to Bill Durham, George Janson, Becky Olson, and Bill Davis for maintaining more than 80 instruments and the complex database. This work was supported under USDA agreement 99-34263-8566 and NASA Contract NCC5-268

REFERENCES

1. J. E. Frederick and D. Lubin, "The budget of biologically active ultraviolet radiation in the Earth-Atmosphere system," *J. Geophys. Res.*, **93**, 3825-3832 1988.
2. S. Madronich, "Implications of recent total atmospheric ozone measurements for biologically active ultraviolet radiation reaching the Earth's surface," *Geophys. Res. Lett.*, **19**, 37-40, 1992.
3. S. Madronich and C. Granier, "Impact of recent total ozone changes on tropospheric ozone photodissociation, hydroxyl radicals, and methane trends," *Geophys. Res. Lett.*, **19**, 465-467, 1992.
4. S. Madronich and F.R. de Gruijl, "Skin cancer and UV radiation," *Nature*, **366**, 23, 1993.
5. T. F. Eck, P.K. Bhartia, and J.B. Kerr, "Satellite estimation of spectral UVB irradiance using TOMS derived total ozone and UV reflectivity," *Geophys. Res. Lett.*, **22**, 611-614, 1995.
6. J. R. Herman, B.K. Bhartia, J. Ziemke, Z. Ahmad, and D. Larko, "UV-B increases (1979-92) from decreases in total ozone," *Geophys. Res. Letter*, **23**, 2117-2120, 1996.
7. J. R. Herman, N. Krotkov, E. Celarier, D. Larko, and G. Labow, "The distribution of UV radiation at the Earth's surface from TOMS measured UV-backscattered radiances," *J. Geophys. Res.*, **104**, 12,059-12,076, 1999.
8. C. S. Long, A.J. Miller, H.T. Lee, J.D. Wild, R.C. Przywarty, and D. Hufford, "Ultraviolet Index forecasts issued by the National Weather Service," *Bull. Amer. Meteor. Soc.*, **77**, 729-747, 1996.
9. R. Meerkötter, B. Wissinger, and G. Seckmeyer, "Surface UV from ERS2/GOME and NOAA/AVHRR data: A case study," *Geophys. Res. Lett.*, **24**, 1939-1942, 1997.
10. D. Lubin, E. Jensen, and H. Gies, "Global surface ultraviolet radiation climatology from TOMS and ERBE data," *J. Geophys. Res.*, **103**, 26,061-26,091, 1998.
11. S. Madronich, R.L. McKenzie, L.O. Bjorn, and M.M. Caldwell, "Changes in biologically active ultraviolet radiation reaching the Earth's surface," *Photochem. Photobiol.*, **46**, 5-19, 1998.
12. B. Mayer, C.A. Fischer, and S. Madronich, "Estimation of surface actinic flux from satellite (TOMS) ozone and

- cloud reflectivity measurements," *Geophys. Res. Letts.*, **25**, 4321-4324.
13. N.A. Krotkov, P.K. Bhartia, H.R. Herman, V. Fioletov, and J. Kerr, "Satellite estimation of spectral surface UV irradiance in the presence of tropospheric aerosols, 1. cloud-free case," *J. Geophys. Res.*, **103**, 8779-8793, 1998.
 14. P. M. Udelhofen, P. Gies, C. Roy, and W.J. Randel, "Surface UV radiation over Australia, 1979-1992: effects of ozone and cloud cover changes on variations of UV radiation," *J. Geophys. Res.*, **104**, 19,135-19,159, 1999.
 15. P. F. Soulen and J.E. Frederick, "Estimating biologically active UV-irradiance from satellite radiance measurements: a sensitivity study," *J. Geophys. Res.*, **104**, 4117-4126, 1999.
 16. P. Wang, Z. Li, J. Cihlar, D.I. Wardle, and J. Kerr, "Validation of an UV inversion algorithm using satellite and surface measurements," *J. Geophys. Res.*, **105**, 5037-5048, 2000.
 17. S. Kalliskota, J. Kaurola, P. Taalas, J.R. Herman, E.A. Celarier, and N.A. Krotkov, "Comparison of daily UV doses estimated from Nimbus 7/TOMS measurements and ground-based spectroradiometric data," *J. Geophys. Res.*, **105**, 5059-5067, 2000.
 18. J. Matthijsen, H. Slaper, and H.A.J.M. Reinen, "Reduction of solar UV by clouds: a comparison between satellite-derived cloud effects and ground-based radiation measurements," *J. Geophys. Res.*, **105**, 5069-5080, 2000.
 19. J. Verdebout, "A method to generate surface UV radiation maps over Europe using GOME, Meteosat, and ancillary geophysical data," *J. Geophys. Res.*, **105**, 5049-5058, 2000.
 20. N. A. Krotkov, J. R. Herman, P. K. Bhartia, V. Fioletov, and Z. Ahmad, "Satellite estimation of spectral surface UV irradiance 2. Effect of homogeneous clouds and snow," *J. Geophys. Res.*, **106**, 11,743-11,759, 2001.
 21. D. S. Bigelow, J. R. Slusser, A. F. Beaubien, and J. H. Gibson, "The USDA Ultraviolet Radiation Monitoring Program," *Bull. Amer. Meteor. Soc.*, **79**, 601-615, 1998.
 22. J. R. Slusser, J. H. Gibson, D. Kolinski, P. Disterhoft, K. Lantz and A. F. Beaubien, "Langley Method of Calibrating UV Filter Radiometers," *J. Geophys. Res.*, 4841-4849, **105**, 2000.
 23. D. S. Bigelow and J. R. Slusser, "Establishing the stability of multi-filter UV rotating shadow-band radiometers," *J. Geophys. Res.*, **105**, 4833-4840, 2000.
 24. J. Gröbner, M. Blumthaler, and W. Ambach, "Experimental investigation of spectral global irradiance measurements errors due to non-ideal cosine response," *Geophys. Res. Letts.*, **23**, 2493-2496, 1996.
 25. K. Stamnes, S. C. Tsay, W. Wiscombe and K. Jayaweera, "Numerically stable algorithm for discrete-ordinate-method radiative transfer in multiple scattering and emitting layered media," *Appl. Opt.*, **27**, 2502-2509, 1988.
 26. S. Madronich, *Environmental Effects of Ultraviolet (UV) Radiation*, chapter: UV radiation in the natural and perturbed atmosphere, Lewis Publisher, Boca Raton, 17-69, 1993.
 27. W. Gao, J. Slusser, J. Gibson, G. Scott, D. Bigelow, J. Kerr, and B. McArthur, "Direct-Sun column ozone retrieval by the ultraviolet multifilter rotating shadowband radiometer and comparison with those from Brewer and Dobson spectrophotometers," *Appl. Opt.* **40**, 3149-3155, 2001.
 28. J. Zeng, R McKenzie, K. Stamnes, M. Wineland, and J. Rosen, "Measured UV spectra compared with discrete ordinate method simulations," *J. Geophys. Res.*, **99**, 23,019-23,030, 1994.
 29. J. Gröbner and J. Kerr, "Ground-based determination of the spectral ultraviolet extraterrestrial solar irradiance: Providing a link between space-based and ground-based solar UV measurements," *J. Geophys. Res.* **106**, 7211-7217, 2001.
 30. R. L. McKenzie, M Kotkamp, W. Ireland, "Upwelling UV spectral irradiances and surface albedo measurements at Lauder, New Zealand," *Geophys Res Letts.*, **23**, 1757-1760, 1996.
 31. L. Harrison and J. Michalsky, "Objective algorithms for the retrieval of optical depths from ground-based measurements," *Appl. Opt.*, **33**, 5126-5132, 1994.
 32. J. R. Herman and E. Celarier, "Earth surface reflectivity at 340-380 nm from TOMS data," *J. Geophys. Res.*, **102**, 28,003-28,011, 1997.
 33. G. E. Shaw, "Sun Photometry," *Bull. Amer. Meteor. Soc.*, **64**, 4-10, 1983.

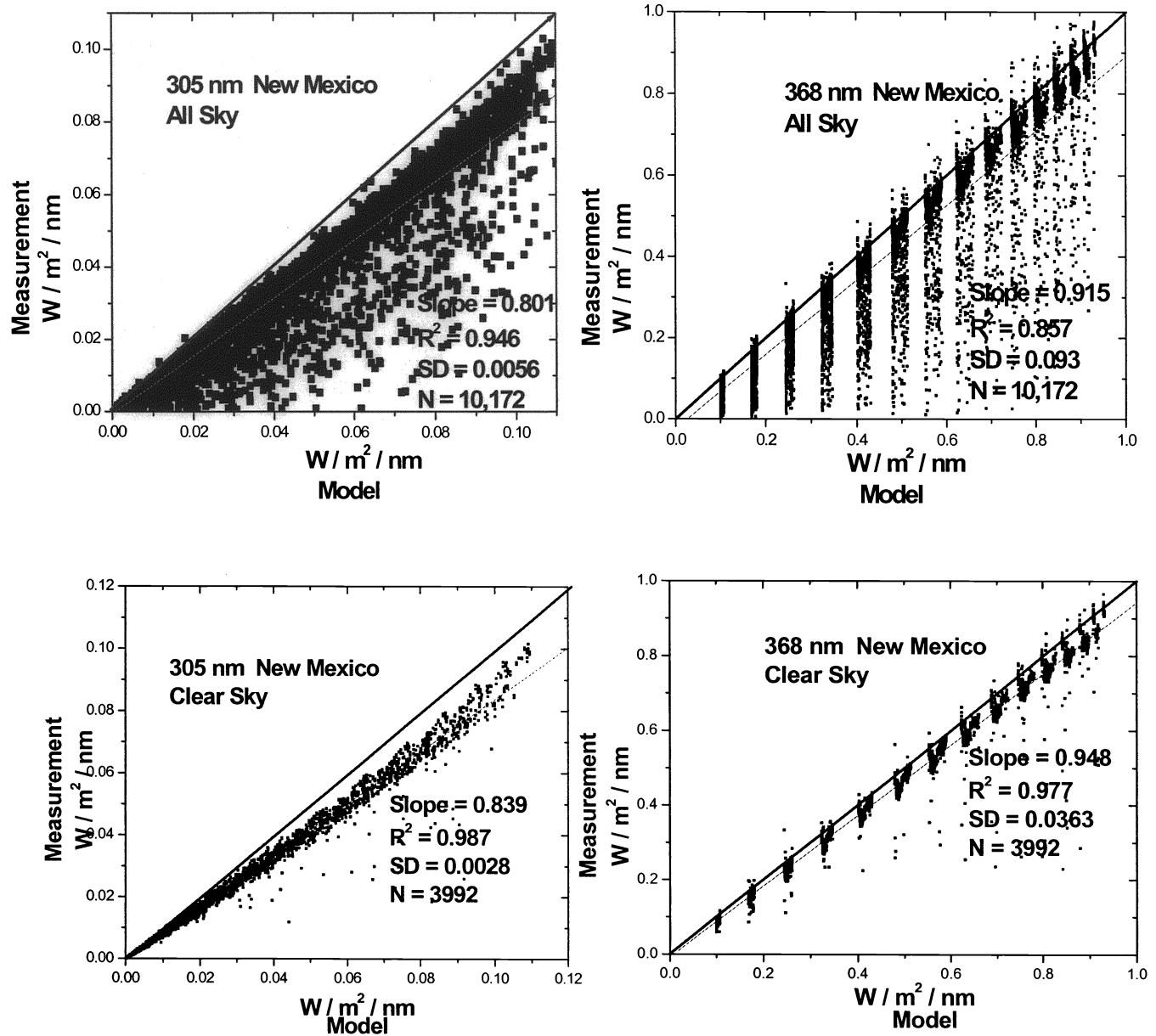


Figure 3: Comparisons of the USDA measurements versus the DISORT model for the New Mexico site. The top left graph is for 305 nm and the top right graph is for 368 nm (both all sky conditions). The bottom left graph shows 305 nm and the bottom right graph shows the 368 nm (both clear sky).

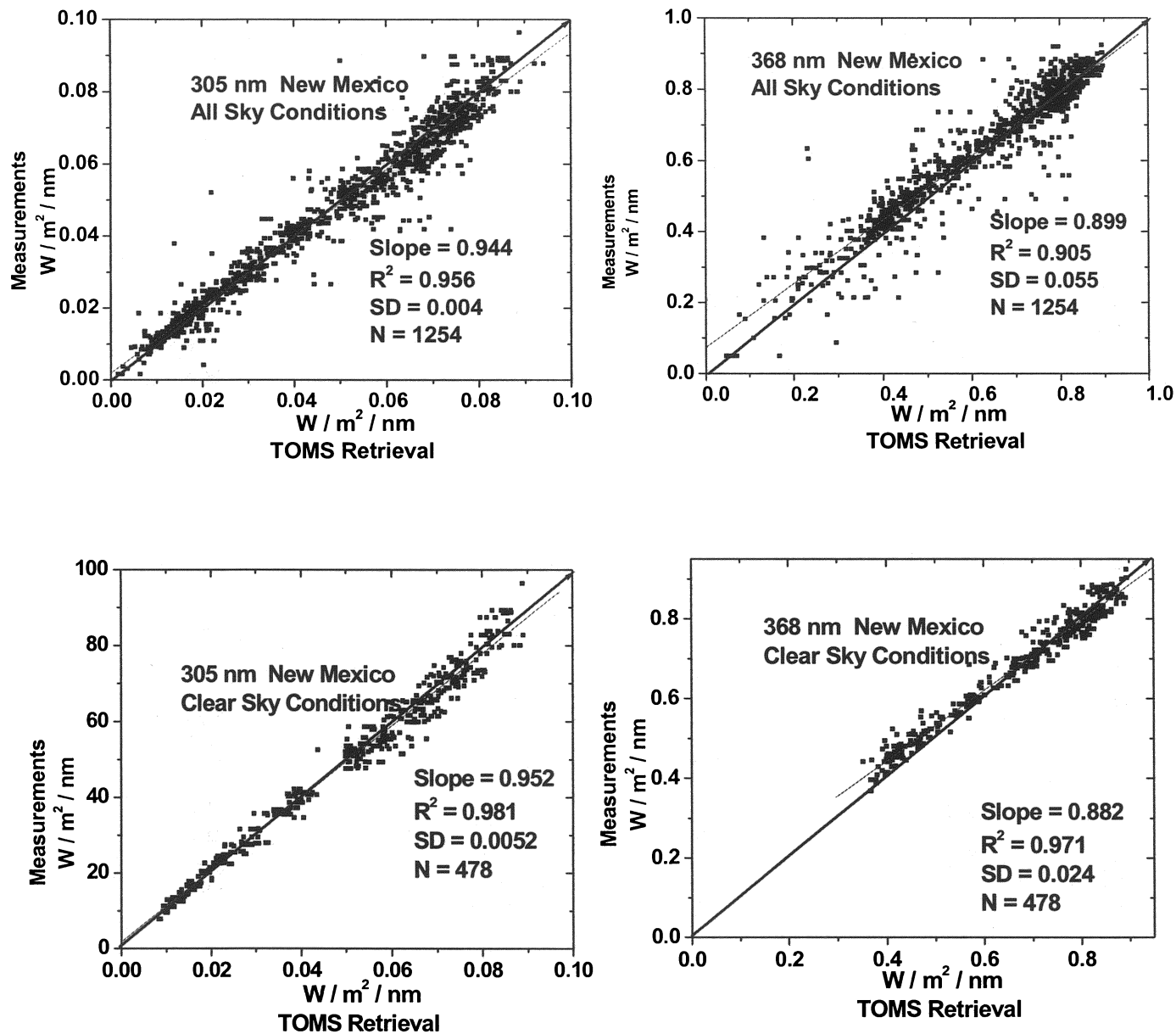


Figure 4: Comparisons of the USDA measurements versus the TOMS retrieval for New Mexico site. The top left graph is for 305 nm and the top right graph is for 368 nm (both all sky conditions). The bottom left graph shows 305 nm and the bottom right shows the 368 nm comparisons (both clear sky).

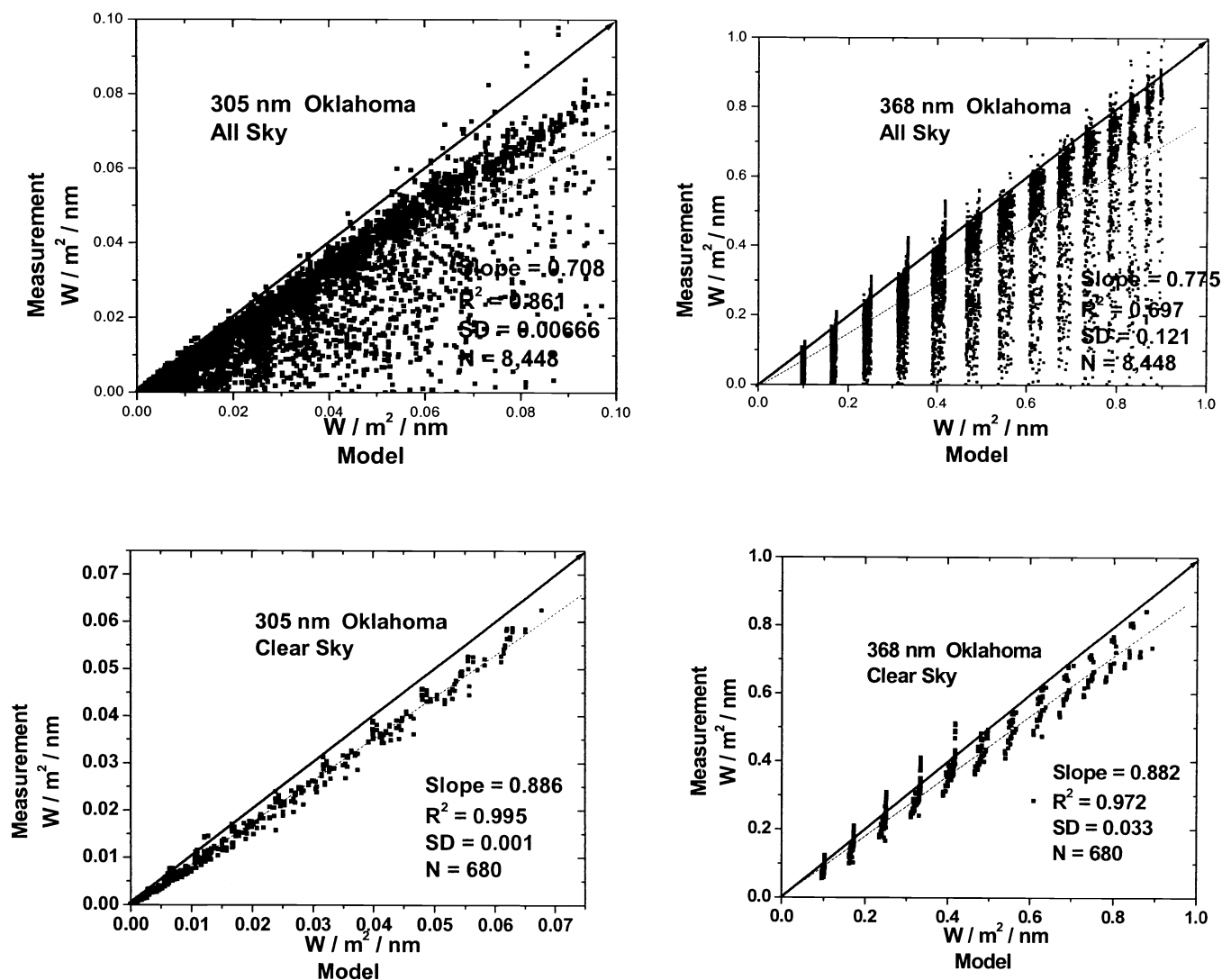


Figure 5: Comparisons of the USDA measurements versus the DISORT model for Oklahoma site. The top left graph is for 305 nm and the top right graph is for 368 nm (both all sky conditions). The bottom left graph shows 305 nm and the bottom right graph shows 368 nm (both clear sky).

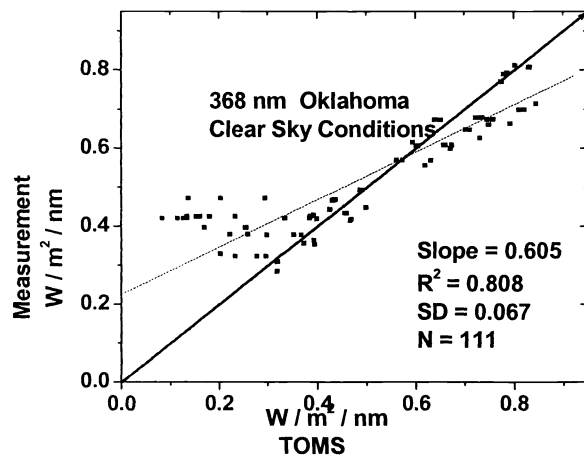
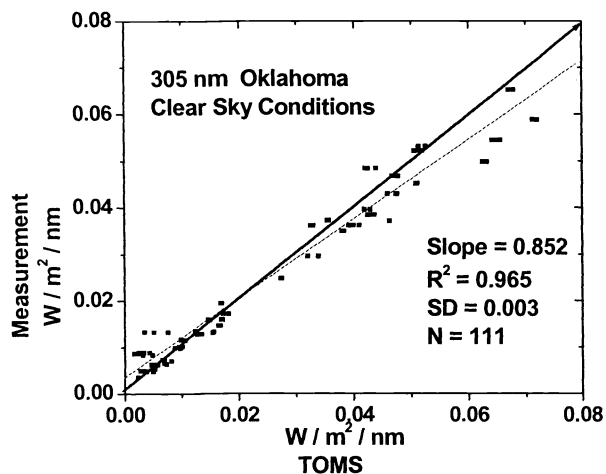
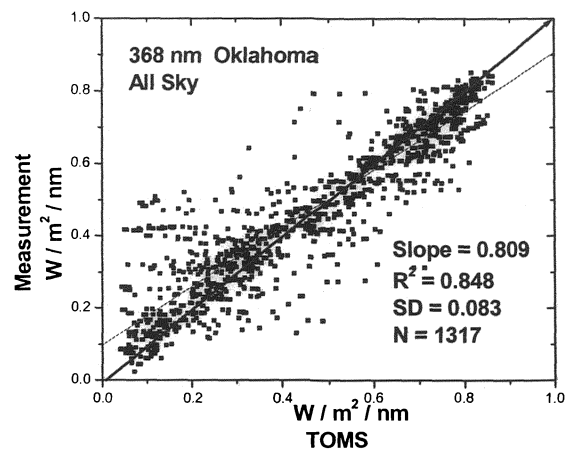
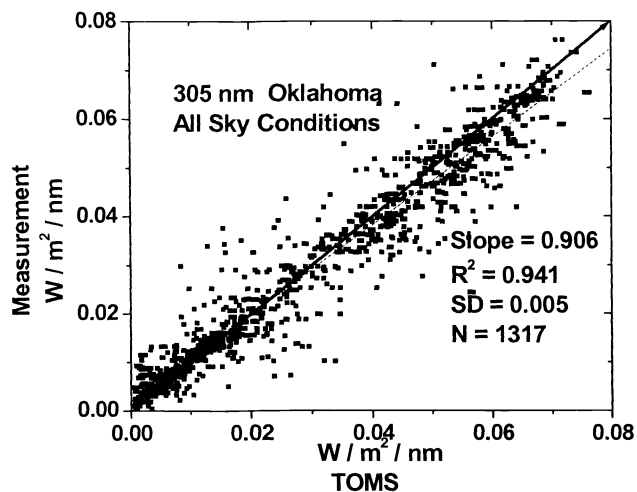


Figure 6: Comparisons of the USDA measurements versus the TOMS retrievals for the Oklahoma site. The top left graph is for 305 nm and the top right graph is for 368 nm (both all sky conditions). The bottom left graph show 305 nm and the bottom right graph 368 nm (both clear sky).

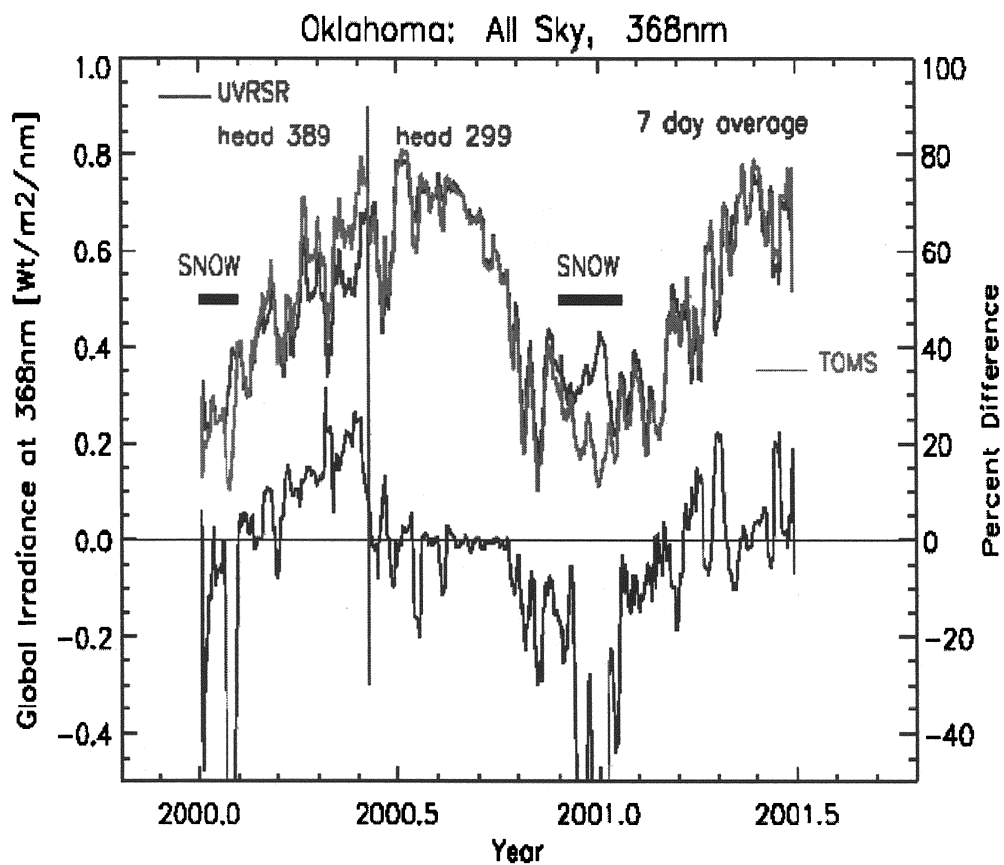


Figure 7: A time series of USDA measurements and TOMS retrievals at 368 nm for the Oklahoma site. Agreement is generally very good except for the snowy periods and near the end of the field cycle of head 389 when the radiometer's sensitivity decreases.

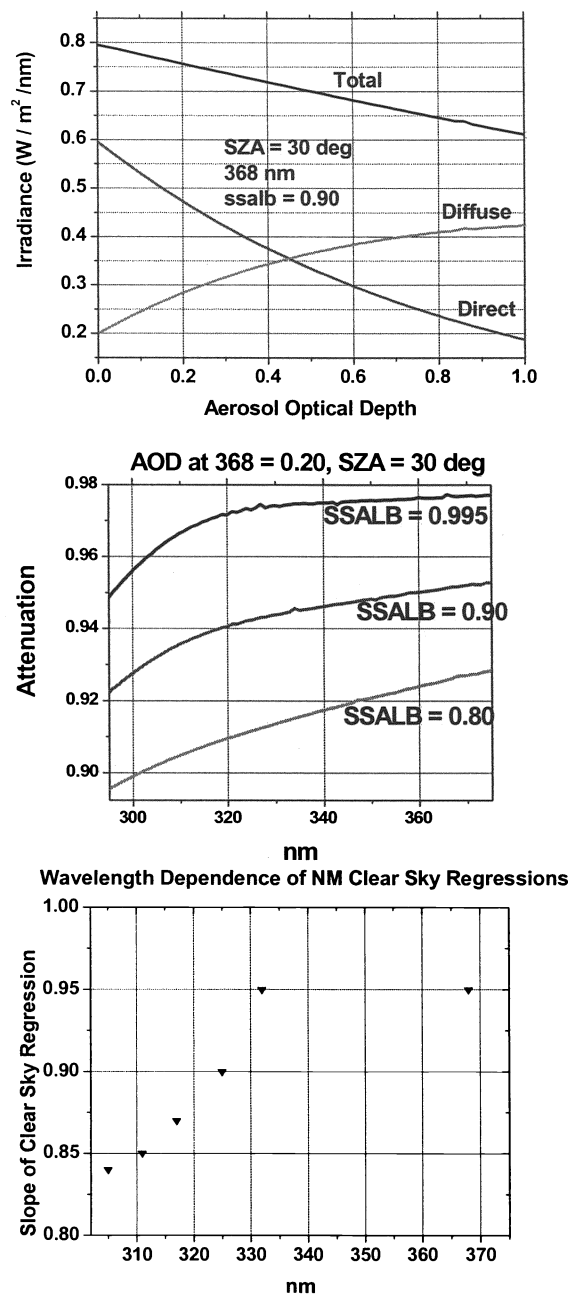


Figure 8: The top graph shows model results of the attenuation due to aerosols of the total, diffuse, and direct horizontal irradiances as a function of aerosol optical depth for a single scattering albedo of 0.90. The middle graph shows the spectral attenuation of the total horizontal irradiance for aerosol optical depth of 0.20 and Ångström exponent of 1 and single scattering albedo of 0.995, 0.90, and 0.80. The bottom graph shows the spectral dependence of the slope of the clear sky regression line of measurements compared with DISORT for the New Mexico site .